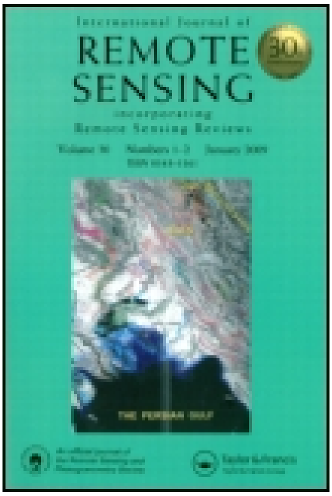

International Journal of Remote Sensing
Publication details, including instructions for authors and subscription information:
http://www.tandfonline.com/loi/tres20

A spaceborne assessment of cyclone impacts on Barents Sea surface temperature and chlorophyll

E. Morozov[ab], D. Kondrik[ac], A. Fedorova[ad], D. Pozdnyakov[ae], D. L. Tang[f] & L. Pettersson[e]

[a] Nansen International Environmental and Remote Sensing Centre, Saint Petersburg, Russia

[b] Department of Ecology, Environment and Plant Sciences, Stockholm University, Stockholm, Sweden

[c] Department of Oceanology, Arctic and Antarctic Research Institute, Saint Petersburg, Russia

[d] Department of Oceanology, Institute of Earth Sciences, Saint Petersburg State University, Saint Petersburg, Russia

[e] Nansen Environmental and Remote Sensing Centre, Bergen, Norway

[f] State Key Laboratory of Tropical Oceanography, South China Institute of Oceanology, Chinese Academy of Sciences, Guangzhou, China

Published online: 07 Apr 2015.

To cite this article: E. Morozov, D. Kondrik, A. Fedorova, D. Pozdnyakov, D. L. Tang & L. Pettersson (2015) A spaceborne assessment of cyclone impacts on Barents Sea surface temperature and chlorophyll, International Journal of Remote Sensing, 36:7, 1921-1941, DOI: 10.1080/01431161.2015.1029098

To link to this article: http://dx.doi.org/10.1080/01431161.2015.1029098

International Journal of Remote Sensing, 2015
Vol. 36, No. 7, 1921–1941, http://dx.doi.org/10.1080/01431161.2015.1029098

Taylor & Francis
Taylor & Francis Group

A spaceborne assessment of cyclone impacts on Barents Sea surface temperature and chlorophyll

E. Morozov[a,b]*, D. Kondrik[a,c], A. Fedorova[a,d], D. Pozdnyakov[a,e], D. L. Tang[f], and L. Pettersson[e]

[a]*Nansen International Environmental and Remote Sensing Centre, Saint Petersburg, Russia;* [b]*Department of Ecology, Environment and Plant Sciences, Stockholm University, Stockholm, Sweden;* [c]*Department of Oceanology, Arctic and Antarctic Research Institute, Saint Petersburg, Russia;* [d]*Department of Oceanology, Institute of Earth Sciences, Saint Petersburg State University, Saint Petersburg, Russia;* [e]*Nansen Environmental and Remote Sensing Centre, Bergen, Norway;* [f]*State Key Laboratory of Tropical Oceanography, South China Institute of Oceanology, Chinese Academy of Sciences, Guangzhou, China*

(*Received 20 October 2014; accepted 24 January 2015*)

A pilot satellite-based investigation of modulations exerted upon mixed-layer phytoplankton fields by cyclones was performed for the first time across a selected part of the Arctic Ocean, the Barents Sea (BS). Resorting to a synergistic approach, cyclones were first identified from NCEP/NCAR data for the summer period during 2003–2013, and their propagation throughout the BS was further surveyed. The above-water wind force was retrieved from QuikSCAT data. These data were further accompanied by ocean colour data from SeaWiFS and MODIS to examine the spatial and temporal distributions of surficial phytoplankton chlorophyll concentration (chl) dynamics along the trajectory of the cyclone's footprint across the sea. Sea surface temperature was retrieved from MODIS data. The specific trajectory of cyclone passage across the BS area, depression depth, and wind speed proved to be conjointly the main factors determining the sign, amplitude, and duration of modulations of phytoplankton chl. The spaceborne data obtained over more than a decade indicate that, on balance, the cyclone passage led to increase in chl within the cyclone footprint area. On average, this increase did not exceed 1–2 μg l^{-1}, which is nevertheless appreciable given that the mean chl within the cyclone footprint rarely exceeded 1 μg l^{-1}. However, chl enhancement within the footprint area lasted only within the range of a few days to a fortnight, with the footprint area generally accounting for about 14% of the BS area. During the vegetation season (April–August, rarely till mid-September), the number of cyclones prone to optical and infrared remote sensing was about 2–3. In light of the above, arguably the cyclones studied are hardly capable of boosting annual primary productivity in the BS. Moreover, it can be conjectured that the same conclusion can be drawn with respect to the pelagic Arctic tracts that are generally less productive and more extensively cloud-covered than the BS. However, this supposition requires further studies in order to advance our understanding of the actual role of cyclones in modulation of Arctic Ocean productivity and ecosystem functioning.

1. Introduction

Among the variety of environmental effects produced by ongoing climate change, significant variations in both primary productivity and time- and area-integrated marine

*Corresponding author. Email: evgeny@niersc.spb.ru

production are becoming increasingly evident (Greene and Pershing 2007; Pabi, van Dijken, and Arrigo 2008; Arrigo et al. 2012; Bélanger, Babin, and Tremblay 2013; Petrenko et al. 2013). Undoubtedly, amply documented shifts in primary production (PP) are a reflection of serious alterations occurring in the ecosystems of the world's oceans (Grebmeir et al. 2006; Loeng and Drinkwater 2007; Byju and Kumar 2011; Yu et al. 2013). Revealed over a wide variety of marine/oceanic regions, these alterations are driven by a host of climate change-related mechanisms hitherto insufficiently understood (Hanshaw, Lozier, and Palter 2008).

Deep baric formations in the atmosphere have been demonstrated capable of markedly affecting PP variations across oceanic/marine tracts (Chang, Chung, and Gong 1996; Lin et al. 2003; Davis and Yan 2004; Tang et al. 2004a, 2004b, 2006; Walker, Leben, and Balasubramanian 2005; Zhao and Tang 2006; Rao, Smith, and Ali 2006; Zheng and Tang 2007; Zhao, Tang, and Wang 2008, 2009; Toratani 2008; Byju and Kumar 2011; Sarangi 2011; Lin 2012; Chung, Gong, and Hung 2012; Chen and Tang 2012; Tang and Sui 2014).

The atmospheric impact on PP is evidenced by a number of satellite-based studies employing synergistic approaches. These studies seemingly indicate that the increase in phytoplankton biomass provoked by cyclones can arise from a variety of waterborne processes (Le Fouest et al. 2011). Predominantly, investigations of cyclone impacts have been conducted over low-latitude waters in the northern hemisphere: the Western North Pacific (reportedly, the area with the highest incidence of tropical cyclones (Webster et al. 2005; Ying et al. 2012)), and, more specifically, the South China Sea as well as the Indian Ocean (Bay of Bengal and Eastern Arabian Sea) and northern Atlantic Ocean (Gulf of Mexico and the 24–38° N latitudinal belt). This interest in specifically studying low-latitude marine/oceanic tracts is accentuated by expectation that the incidence of tropical cyclones will steadily rise with ongoing climate warming (Knutson et al. 2010; Ying et al. 2012).

There are reasons to assume that the effect of deep cyclones on PP in the Arctic Ocean can also be appreciable/consequential (Le Fouest et al. 2011), regardless of the fact that it is a somewhat low-production region among the world's oceans (Arrigo and van Dijken 2011). We are unaware, however, of any satellite-based investigations of this phenomenon at these latitudes.

Although Arctic Ocean ecosystems are subject to atmospheric and hydrodynamic forcing of a different nature (Bobylev, Kondratyev, and Johannessen 2003), identification of the specific role of deep cyclones in PP variation and quantification of the ensuing consequences is a feasible task due to the specific spatial and temporal scales inherent in this driving mechanism. Indeed, when studying, for example, the Nordic seas, the relevant scales are of a few hundred kilometres and a few days, which are not characteristic of many other examples of external forcing (Yu 2009).

Although achievable, the above task must be considered challenging because of the high incidence of heavy cloud conditions over ice-free tracts of the Arctic (Chernokulsky and Mokhov 2012). This necessitates the application of spatio-temporal averaging of data in the visible which, inevitably, will affect the spatio-temporal resolution of spaceborne images and thus complicate the quantitative assessment of cyclonic impact on PP. Obviously, a reasonable trade-off should be found to overcome this impediment.

Since, in comparison with low-latitude productive waters, variation in PP levels in the Arctic is relatively small, the retrieval error can be significant (Petrenko et al. 2013) and this imposes strict requirements of the inference of the desired information. A solid statistical substantiation of the data is a prerequisite in this case.

To increase the analytical capacity of the research, a synergistic approach is required in order to consider not solely the ocean colour data (from which phytoplankton chlorophyll concentration (chl) and PP are retrievable), but also sea surface temperature (SST) and near-surface winds, as well as currents, frontal zones/zones of convergence and divergence, the bathymetry of the target region, and meteorological data on the baric fields.

Below we present the results of our pilot study aimed at revealing and quantitatively assessing the impact of cyclones on phytoplankton chl and SST spatial and temporal variation in the Arctic. At this stage of the research, the target region was confined to the Barents Sea (BS) and the period covered was 2003–2013. This areal limitation did not permit us to make any generalized conclusions regarding the role of cyclones in PP dynamics across the whole of the Arctic Ocean; we intend to address this at subsequent stages of the research.

2. A concise overview of previous studies

Storm-induced perturbations in the thermohydrodynamic state of the upper ocean were revealed and theoretically investigated in the 1960s (Leipper 1967). In the early 1980s, airborne means were employed to study the aftermath of hurricane passage – first and foremost, spatio-temporal changes in SST.

By the early 1990s, spaceborne thermal remote sensing had largely replaced aeroplane-based observation. In the early 2000s, a synergistic remote-sensing approach began to be exploited to widen the range of variables characterizing this multifaceted phenomenon, when phytoplankton biomass dynamics was found to be one of the most important and highly consequential after-effects of hurricane translation over oceanic/marine tracts (Robinson 2004).

As mentioned above, previous studies of storm-driven impacts on the upper ocean were almost entirely confined to low latitudes, which are the realm of tropical cyclones/hurricanes/typhoons (Tang and Sui 2014). The latitudinal belt within which investigations have mostly been performed extends between 4° N and 30° N (see relevant references in the Introduction) with the only exception being the Sea of Okhotsk (45–50° N), which has also been studied in connection with the invasion of tropical cyclones (Permyakov et al. 2005; Kawai and Wada 2011; Akmaykin et al. 2013; Salyuk, Golik, and Stepochkin 2014). Similar reports from the southern hemisphere oceans are scarce and mainly target various issues relating to SST (see, e.g. Price, Sandford, and Forritall 1994; Dare and McBride 2011; Jullien et al. 2012).

The studies cited above reveal that maximum rainfall and SST cooling are, respectively, on the left and right sides of the cyclone track. Moving cyclones cause (1) subduction of the upper quasi-homogeneous layer down to several tens of metres; (2) deepening of mixed-layer depth; (3) a rise in PP and CO_2 efflux (outgassing) from the ocean to the atmosphere; and (4) elevation of sea surface.

These perturbations are thought to be driven by a variety of mechanisms: (1) wind mixing (followed by upward Ekman pumping); (2) transient upwelling; (3) entrainment; (4) movement of subsurface chl to the ocean upper layer; and (5) rapid ventilation of the thermocline and nutricline.

The level of perturbation caused by moving tropical cyclones is case/area-specific and varies within a wide range. Thus the increase in chl, and correspondingly PP, reported from the North Atlantic (Hanshaw, Lozier, and Palter 2008) was insignificant, whereas in the Northwest Pacific typhoon activity contributed 0.4–40% of summer/fall production (Siswanto et al. 2007). In 2012, also in the North Atlantic, PP reportedly increased by 0.15% due to cyclones. Interestingly, Lin (2012), investigating 11 cyclones, found that the most severe cyclone produced no increase in PP. Byju and Kumar (2011) communicated their finding that a hurricane in the Bay of Bengal led to a relatively low increase in chl (~0.5 mg m^{-3}) but a twofold increase in PP. Rao, Smith, and Ali (2006) reported an approximate cumulative fivefold increase in PP in the same area due to cyclones, with increase in chl varying from four- to ninefold. A 2.5- to 3-fold increase in chl was established by Walker, Leben, and Balasubramanian (2005) in the Gulf of Mexico. Babin et al. (2004) previously determined that within the subtropical coastal zone of the USA, chl increased in the range 5–91% due to strong cyclones. In the South China Sea, increases of 30- to 40-fold, and even 60-fold, in chl were recorded, with PP increments during typhoon periods being 3.5% (Lin et al. 2003; Zheng and Tang 2007; Zhao and Tang 2006; Zhao, Tang, and Wang 2008). Kawai and Wada (2011) found that in the waters south of Japan, in the Sea of Okhotsk and in the regions between 35° N and 45° N, especially in the Kuroshio–Oyashio Extention (KOE) region, the contribution of cyclones to annual increase in chl was generally small: cyclone-induced chl increase accounted for only a small percentage of total chl increase in some areas. However, short-term increases accompanied by cyclones provoked 10–30% of the accumulated chl increase, or more, in the South China, East China, Yellow, and Japan Seas as well as in the Sea of Okhotsk.

Water cooling due to cyclone passage varied within the range −2 to –9°C: −2.5 to −6°C in Northwestern Pacific (Lin 2012), –1 to −2°C in the Arabian Sea (Byju and Kumar 2011), −2 to –3°C in the Bay of Bengal (Rao, Smith, and Ali 2006; Sarangi 2011), −3 to −7°C in the Gulf of Mexico (Walker, Leben, and Balasubramanian 2005), and −5 to −9°C in the South China Sea (Zheng and Tang 2007; Lin et al. 2003).

The lag time between cyclone passage and ensuing SST and chl reaction ranged between 3 and 9 days: 7–9 days in the North Pacific (Akmaykin et al. 2013); 7 days near the Pearl River estuary and in the Bay of Bengal (Zhao, Tang, and Wang 2009; Rao, Smith, and Ali 2006); 3–4 days in the Arabian Sea (Byju and Kumar 2011); 3–4 days in the Gulf of Mexico (Walker, Leben, and Balasubramanian 2005); and 3–6 days in the South China Sea (Lin et al. 2003).

The duration of the effect was also found to be highly variable, ranging between under 2 weeks to one month (Akmaykin et al. 2013; Babin et al. 2004; Lin et al. 2003; Zhao, Tang, and Wang 2009; Kawai and Wada 2011).

Perturbations of SST and chl fields increase with the strength of the above-water wind (V); Akmaykin et al. (2013) reported that this effect became noticeable at $V > 33$ m s^{-1}; Hanshaw, Lozier, and Palter (2008) found that an increase in wind speed in the North Atlantic from 16 to 54 m s^{-1} resulted in a chl response 15% greater; Babin et al. (2004) reported for the Sargasso Sea that an increase in wind speed from 40 to 60 m s^{-1} led to a 20% higher chl response.

Summing up the findings reported in the publications discussed above, it is possible to generalize that the conditions favouring the impact of hurricanes on SST and chl are: deep atmospheric depression (950–980 mb); strong, sustained winds above the water surface; low cyclone translation velocity; large cyclone size; absence of warm eddies within the trajectory of the cyclone's footprint; low mixed-layer depth (MLD); and low depths of thermocline and nutricline. The impacts are reduced if two cyclones move consecutively.

This very brief overview demonstrates that the interplay of both atmospheric and oceanic hydrodynamic conditions explains the actual changes in both SST and chl to the impact of very strong storms.

3. The BS: a general description

The BS is a marginal sea of the Arctic Ocean located off the northern coasts of Norway and Russia (see Figure 1). The BS is bordered by the shelf edge of the Norwegian Sea to

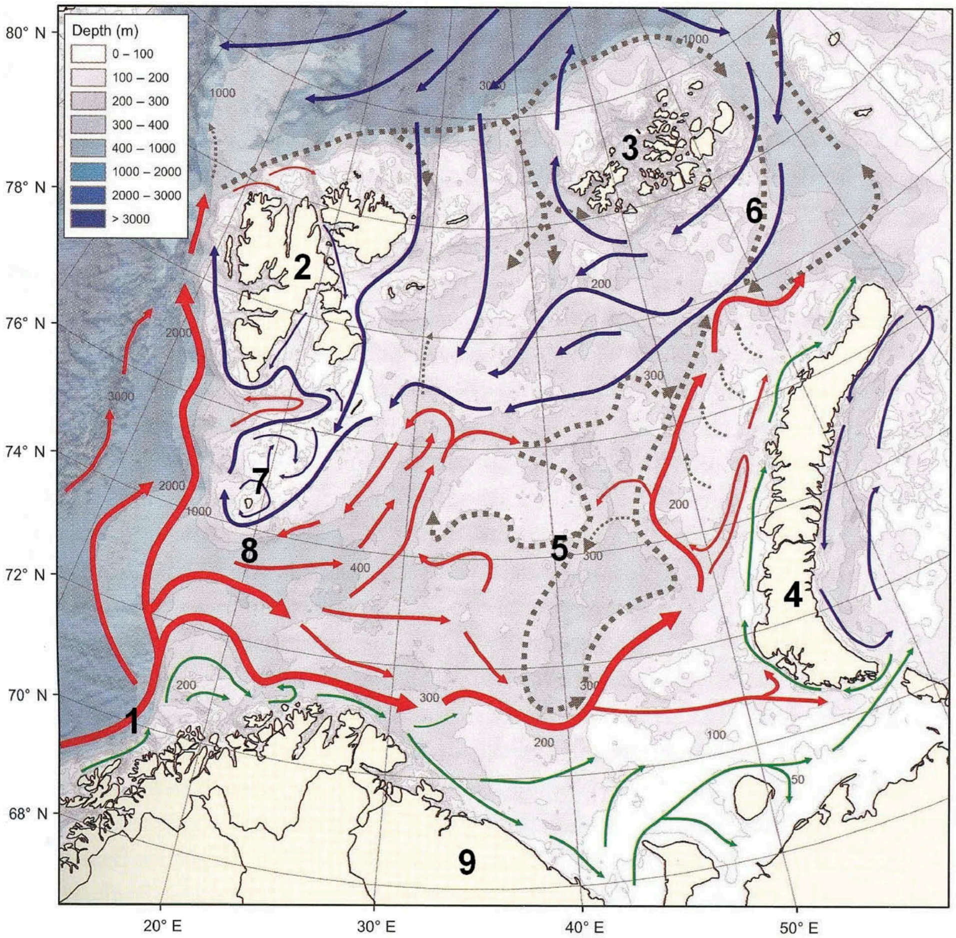

Figure 1. The principal system of currents in the BS. Red, blue, and green arrows denote water flows of Atlantic, Arctic, and coastal zone origin; dotted lines correspond to subsurface currents (Jakobsen and Ozhigin 2011). 1, 2, 3, 4, and 5 designate, respectively, the shelf edge of the Norwegian Sea, the Svalbard Archipelago, Franz Josef Land, the Novaya Zemlia, and the central point of the BS. 6, trough of St. Anna; 7, Bear Island; 8, Barents Gates; 9, the Kola Peninsula. Numbers in small font are depths in metres.

the west, the archipelagos of Svalbard to the northwest, Franz Josef Land to the northeast, and the Novaya Zemlia, with the central point located at 75° N 40° E. The morphometry of the BS is very uneven: the average depth is ~300 m plunging to a maximum of 600 m in the major Bear Island trench.

Due to its geographical layout and specific morphometric features, the BS plays an exceptionally important role in determining the general thermohydrodynamic and hydrobiological conditions across the Arctic Basin (Skagseth et al. 2008).

There are three main types of water mass in the BS: warm, salty Atlantic water (temperature > 3°C, salinity > 35 psu) from the North Atlantic drift, cold Arctic water (temperature < 0°C, salinity < 35 psu) from the north, and warm, but not very salty, coastal water (temperature > 3°C, salinity < 34.7 psu).

The BS is characterized by a relatively shallow shelf and fairly complex hydrography: it is subjected to the very strong dynamic influence of both the Arctic Basin and the Atlantic waters, and thus constitutes an arena of very intricate hydrodynamic interactions of water currents (Figure 1). The main water exchange route is between the Barents Gates and the Saint Anna Trough.

Between the Atlantic and polar waters, a front called the Polar front (PF) is a permanent feature. In summer it is located at 78–80° N extending amid the BS between the Svalbard Islands and the southern coast of Novaya Zemlia. In the western parts of the sea (close to Bear Island), this front is determined by the bottom topography and is therefore relatively sharp and stable from year to year, while in the east (towards Novaya Zemlia) it can be quite diffuse and its position may vary considerably over time. In spring, the PF structure is frequently affected by mesoscale eddies typically 25–40 km, with water vertical velocity measuring 20 md^{-1}.

As the PF enhances the vertical and horizontal mixing in the region, and hence channels the nutrients up to the euphotic zone, it is a site of high biological activity largely explaining that, compared with other marine waters of similar latitude, the BS is a relatively productive high-latitude marine ecosystem.

Tidal/ebbing water motion is significant in the BS, with the tidal amplitude and current direction varying greatly. The atmospheric cyclonic activity over the BS is very pronounced throughout the year.

A significant part of the BS is annually ice-free. In winter (March is the coldest month in the BS basin), the ice edge is located at ~75° N in the northern and western BS confines. However, in the eastern periphery zone, the ice frontier turns abruptly to the south reaching the Kola Peninsula coast. This pattern persists till April and even May. During March an inflow of warm, saline Atlantic water with the Norway Current and their blending with cold and less saline Arctic waters makes this sea very sensitive to atmospheric, hydrodynamic, and, ultimately, climate change forcing (Reigstad et al. 2002) (see Figure 2). In June–September the ice edge has a latitudinal placement closer to ~77–80° N (Jakobsen and Ozhigin 2011).

The climatic index of the BS reveals significant inter-annual variation and a non-linear trend. However, over the last three to four decades there is a distinct trend of climate warming (Jakobsen and Ozhigin 2011).

In regard to the hydrobiology at low trophic levels, phytoplankton development does not last long (April–August, very rarely till mid-September); the phytoplankton composition is rather variable. Depending on the ice regime, daylight duration, and availability of nutrients, the phytoplankton community encompasses algae from classes of Bacillariophyta (predominantly), but also Haptophyta, Dynophyta, as well as dinoflagellates (*Ceratium*).

Over recent decades there have been regular reports (although not necessarily each year) on blooms of a coccolithophore, *Emiliania huxleyi*, in the central and southern regions of the BS. These blooms were observed most frequently in August. They play a very import role in forming inorganic carbon pools in the BS (Smyth, Tyrrel, and Tarrant 2004; Petrenko et al. 2013), and are thought to be among relevant climate change factors.

The BS surface chl during the vegetation period (April–August, rarely till mid-September) is generally below 1.0–1.5 μg l^{-1} except for the marginal ice zone (MIZ), where it can be in the range ~5 to 15 μg l^{-1} and even higher (Engelsen et al. 2002).

SST across the BS during the warm period generally varies longitudinally: the climatological values of SST in June are about −2ºC at the northern boundary of the BS

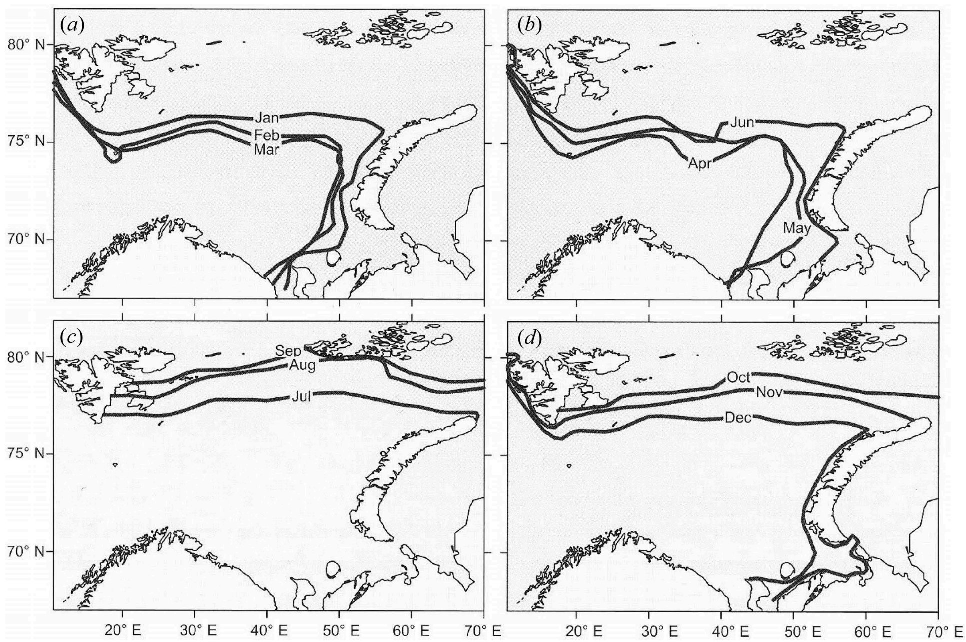

Figure 2. Mean median position of the ice edge in the BS during the first (*a*), second (*b*), third (*c*), and fourth (*d*) quarters. Period of averaging: 1951–2008 (Jakobsen and Ozhigin 2011).

and +5 to +6ºC within the Norwegian and Russian coastal zones of the Kola Peninsula (NOAA ATLAS 2004), whereas in September the respective values are 0ºC and +7 to +8ºC (NOAA ATLAS 2004; NODC 2014).

4. Sources of data

The occurrence of cyclones moving across the BS was determined using the reanalysis data on the geopotential of the 1000 mbar isobaric surface (http://www.esrl.noaa.gov/psd) from the National Centers for Environmental Prediction/National Center for Atmospheric Research (NCEP/NCAR) (Kalnay et al. 1996).

Satellite data on wind speed and direction over the ocean are derived from the National Aeronautics and Space Administration (NASA) based on QuikSCAT data (http://winds.jpl.nasa.gov/missions/quikscat/index.cfm). The spatial resolution of the QuikSCAT and NCEP/NCAR data are, respectively, 25 km and 2.5° (~275 km), with a revisiting frequency of about twice and four times per day, respectively. At wind speeds in the range 3–30 m s^{-1} the accuracy of wind speed and direction is reportedly ~10% (i.e. better than 2 ms^{-1}), and 20º, respectively (Callahan and Lungu 2006).

Ocean colour data were downloaded from three satellite sensors: Sea-viewing Wide Field-of-view Sensor (SeaWiFS) and Moderate-Resolution Imaging Spectroradiometer (MODIS, on Aqua & Terra; http://oceancolor.gsfc.nasa.gov) at spatial resolutions of 1.0 and 1.1 km, respectively, and revisiting frequencies of 2–3 and 4–6 times per day for SeaWiFS and MODIS, respectively. Ocean colour data from SeaWiFS and MODIS (conjointly on Aqua and Terra) were blended daily to obtain a composite image for each specific day. The accuracy of chl data (restored with the standard OC4 and OC3 algorithms, see below) is reportedly ~30% (O'Reilly et al. 1998). To obtain seasonal chl variation, chl data were averaged in each pixel over 10 days through the vegetation period for the entire BS. The accuracy of chl data retrieved with the BOREALI algorithm (Korosov et al. 2009) for areas of coccolithophore blooms is assessed as ~35% (Petrenko et al. 2013).

In addition to ocean colour data, MODIS sensors also provide SST data at spatio-temporal resolution equalling that used for chl fields. The SST data daytime error is assessed at 0.65–0.70 K (Hosoda et al. 2007).

5. Methodology

5.1. Algorithms

5.1.1. Chl standard retrieval algorithm

The concentration of chl was retrieved using the NASA standard algorithms OC4 for SeaWiFS (O'Reilly et al. 1998) and OC3 for MODIS Aqua and Terra (O'Reilly et al. 2000). These are modified cubic polynomial functions based on the band ratio paradigm and employing remote-sensing spectral reflectance in the visible and near infrared channels as the input parameter. The NASA data reprocessed only recently were employed in the present study: reprocessed R2012 and R2010 in the case of MODIS-Aqua, and MODIS-Terra and SeaWiFS, respectively (http://oceancolor.gsfc.nasa.gov/WIKI/OCReproc.html).

5.1.2. SST standard retrieval algorithm

To determine SST, 'window-split' retrieval algorithms were employed. These are based on the difference between the satellite-observed water surface *apparent* (*brightness*) temperature, T_i determined in two several spectral channels centred at 11 μm (T_{11}) and 12 μm (T_{12}). The NASA algorithm is a four-term expression with proportionality coefficients $c_1 - c_4$: $\mathrm{SST} = c_1 + c_2T_{11} + c_3(T_{11} - T_{12}) + c_4[(\sec\phi - 1)(T_{11} - T_{12})$, where ϕ is the satellite zenith angle (http://yyy.rsmas.miami.edu/groups/rrsl/pathfinder/Algorithm/algo_index.html#algo-pathsst and http://modis.gsfc.nasa.gov/data/atbd/atbd_mod25.pdf) (Robinson 1994).

5.1.3. Wind speed standard retrieval algorithm

The concept of wind speed measurements is based on the backscattering of QuikSCAT-transmitted microwave pulses by the water surface. The backscattered microwave signal is modified by the wind-roughened surface in a certain (logarithmic) proportion to the wind speed and direction. Application of inverse modelling allows retrieval of the desired wind parameters (e.g. Gaston and Rodriguez 2008). The reported accuracy of wind speed retrieval is given above.

5.1.4. BOREALI algorithm

It is known that at the final stage of the life cycle, *E. huxleyi* cells liberate into ambient water millions of calcium carbonate plates (called coccoliths). Also, diatoms are known to coexist in the *E. huxleyi* bloom area, although in quantities usually not exceeding 10% of *E. huxleyi* biomass (Thiersten and Young 2004). Based on the Levenberg–Marquardt multivariate optimization procedure (for reference, see Korosov et al. 2009), the

BOREALI algorithm employs a hydro-optical model accounting for the optical impact of (1) the spectral optical properties of *E. huxleyi* cells and coccoliths, (2) diatoms, and (3) water *per se*. The hydro-optical model is designed to make use of the relevant data reported in the literature (for references, see Petrenko et al. 2013; Morozov et al. 2013). This procedure thus assures a simultaneous retrieval of chl from both *E. huxleyi* and coexisting diatoms as well as coccoliths. In our estimation of chl within *E. huxleyi* blooms, the total chl of diatoms and coccolithophores was used.

A preliminary identification of *E. huxleyi* bloom occurrence was based firstly on the turquoise colour of red–green–blue images in algal bloom areas, and secondly on the analysis of the reflectance spectral features using the approach suggested by Morozov (2013) and Morozov et al. (2013). The indicative signatures include (1) enhanced reflection in the blue part of the spectrum and (2) a major pick at ~510 nm (the value of subsurface remote-sensing reflectance is > (0.05–0.07 sr^{-1})) followed by a secondary maximum at ~555 nm and a rather *rapid* decline in the red.

5.2. Selection of cyclones suitable for analysis, and database development

Using the NCEP/NCAR data on the cyclone track, a strip of about 200 km width centred at the cyclone's 'eye' was selected from the colour image(s) of the BS and processed to yield the chl and SST field within the strip. We then selected cases for which the cloud-free area of the moving cyclone footprint strip (200 km wide) accounted for more than 20% of the total strip area. In addition, it was decided that the time of the cyclone passage across the BS should not exceed 3 days because, in the case of more slowly moving cyclones, the ensuing chl field modulation proved to be poorly identifiable. Understandably, we considered only cyclones passing over the BS during the vegetation period.

Ocean colour and infrared (IR) images were acquired and processed for periods of 5 days prior to the advent of the cyclone within the confines of the BS, and for about 10 days after definitive cyclone departure from the target marine zone. In the case of a tandem cyclone arriving at the BS, the changes triggered by both were assessed in a similar way but the period used for averaging was dependent on the time interval between the passage of two baric formations.

To mitigate the screening effect due to cloudiness, the retrieved chl fields were blended from the ocean colour sensors flying over the BS during the cyclone passage, and averaging from once daily to every few days was performed; the exact time period of averaging was prompted in each case by the specific features of cloud coverage.

The database collected also accommodated information about baric pressure/depression depth in the centre (the 'eye') of the cyclone, as well the speed and direction of above-water surface wind at a height of 10 m. The entire spatio-temporal synchronized data were used synergistically for further analysis.

6. Results and discussion

Nearly one hundred cyclones passing over the BS between early April and late August–early September were registered for the period 2003–2013. As illustrated in Figure 3, the monthly number of cyclones rarely exceeded three. Of the overall number of cyclones (96) only 23 were suitable for analysis (according to the criteria specified in Section 5.2).

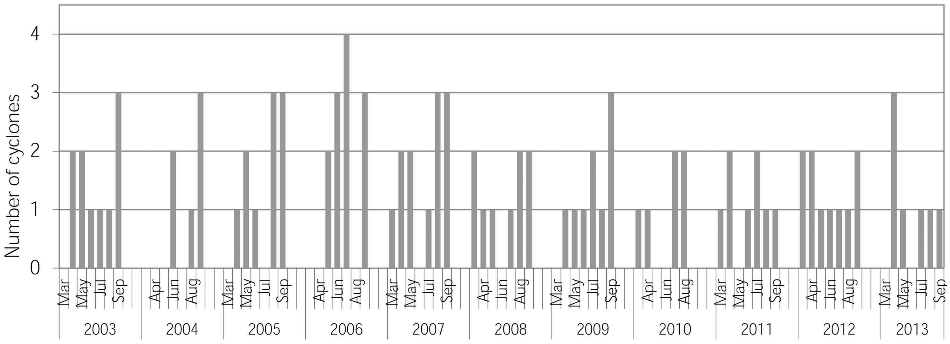

Figure 3. Monthly number of selected cyclones over the BS during the period 2003–2013.

The geopotential height of the 'eye' of the 23 selected cyclones varied in the range −187 to −9 GPM. The maximum wind speed above the water surface varied within the range 13–30 m s^{-1} and the cyclone translation velocity ranged 3–28 m s^{-1}. Figure 4 illustrates the zones of the cyclone tracks within which the cyclone parameters met the requirements formulated in Section 5.2.

The direction of propagation of all 23 cyclones was predominantly from west to east. Most traversed the BS within the region between southern Spitsbergen and the coastal zone of the Kola Peninsula to eventually exit through a corridor extending from mid- to southern Novaya Zemlya. A smaller number exited the BS waters, moving over the summer PF zone (see Figure 4).

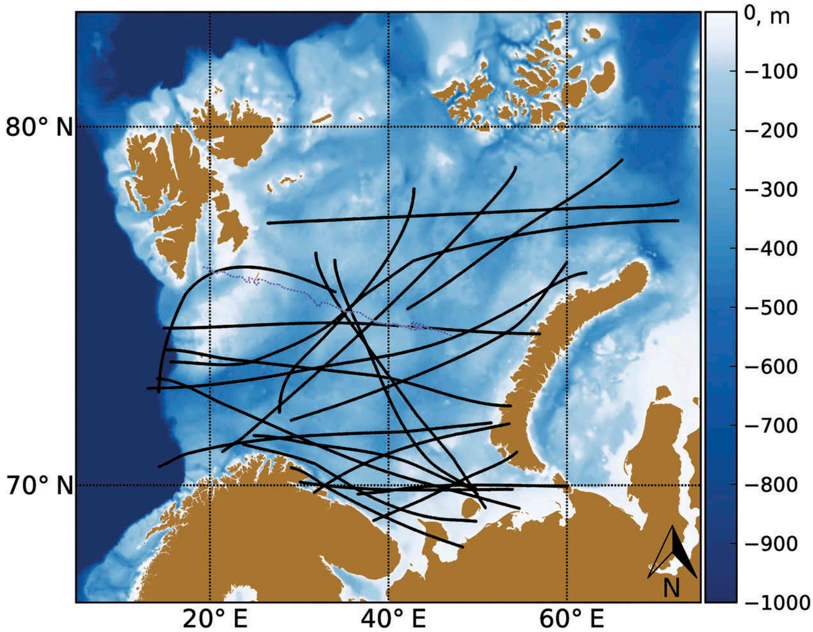

Figure 4. Analysed parts of the considered cyclone tracks, within which the cyclone parameters met the requirements formulated in Section 5.2. Dotted line denotes the summer location of the polar front as reported by Reigstad et al. (2002) for July 1999.

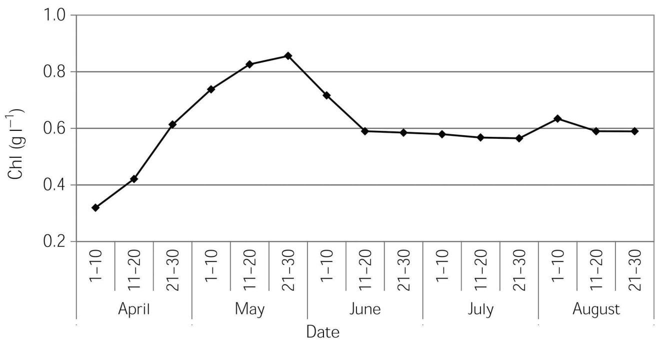

Figure 5. Seasonal variation in chl averaged over 10 days and the entire BS area for the period 2003–2013.

Our spaceborne estimations indicate that the intra-seasonal distribution of cyclone incidence is relatively even – the major cases occur during July–September, but in the latter half of September increase in chl is zero.

It was also found that the distribution of monthly chl averaged over the entire BS exhibited one main peak in late May–early June and a secondary spike in August (Figure 5). Thus, in our analyses we considered the cyclones passing over the BS between April and mid-September assuming this time interval as the BS vegetation season. There is just one caveat: the absolute values and the placement of the maximum in Figure 5 do not account for chl abundance and temporal dynamics in immediate proximity to the ice edge. This was done in order to avoid the inaccuracies inevitably arising from the adjacency effect (Sterckx, Knaeps, and Ruddick 2011).

It was found for all (i.e. 23) selected cyclones that the fraction of the BS surface covered by the strip of the moving cyclone footprint varied between 5% and 28%, with an average value of about 14%.

Our analysis of chl and SST response to moving cyclones indicates that there are two major types of variation pattern typical of the BS. The first of these is characterized, first, by a decrease in chl followed by an increase (exemplified in Figure 6).

As illustrated in Figure 7, the second pattern exhibits a brief increase in chl as well as in SST that is succeeded, first, by a further increase in both variables then a decrease, and finally a near restitution of initial values (i.e. prior to cyclone passage).

The incidence of responses of the first type is more frequent: 17 of the 23 cyclones observed and analysed. For both response types with respect to the direction of cyclone translation, a more intense surface chl enhancement (up to 25%) was observed in the right-hand side of the footprint strip.

Statistical analysis of the multiple linear regression (MLR) model for chl enhancement (+Δchl, μg l^{-1})) produced by moving cyclones indicates that it significantly ($p < 0.002$) correlates with both depression depth (H, GPM) and cyclone translation speed (V, m s^{-1}) and with a coefficient of determination of 0.75 (RMSE = 0.029 (or 16.6%)):

$$+\Delta\text{chl} = 0.18 + 0.0052H - 0.0007V. \quad (1)$$

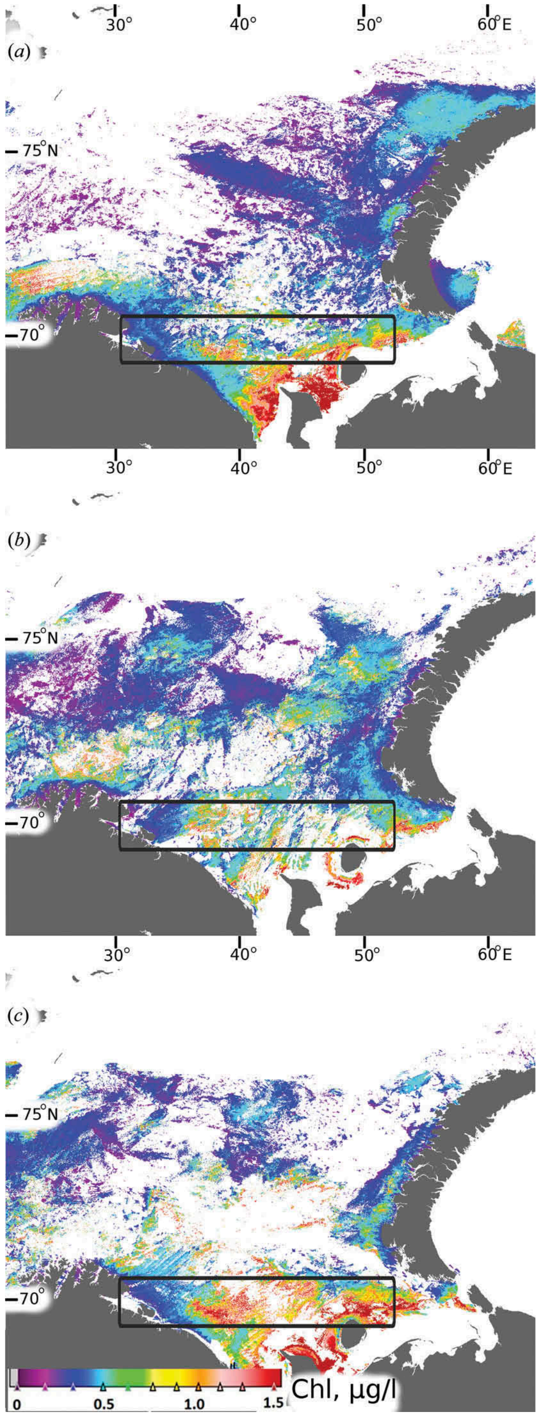

Figure 6. The Barents Sea, 13–14 April 2012. Spatial distribution of surface chl averaged within the cyclone footstep area over (*a*) the days 1–5 prior to cyclone passage, (*b*) days 1–5 after the cyclone passage, and (*c*) days 6–10 after the cyclone passage. (*d*) Illustrates the temporal variation in, respectively, chl and SST; points A and B on the abscissa designate the period, respectively, 5 days prior to cyclone arrival and 5 days (from days 6–10) after cyclone departure.

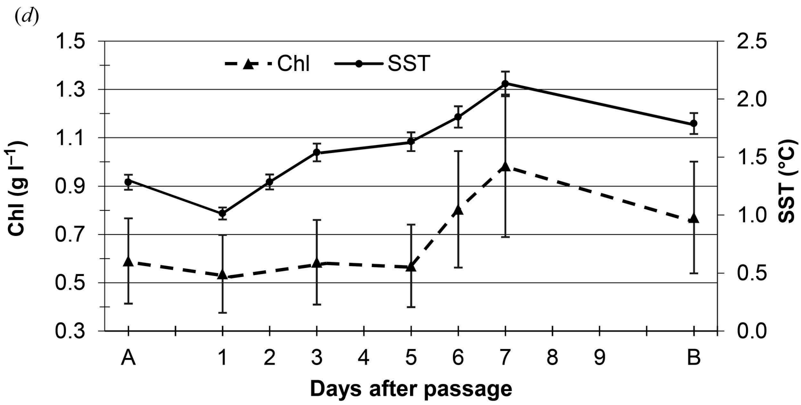

Figure 6. (*Continued*)

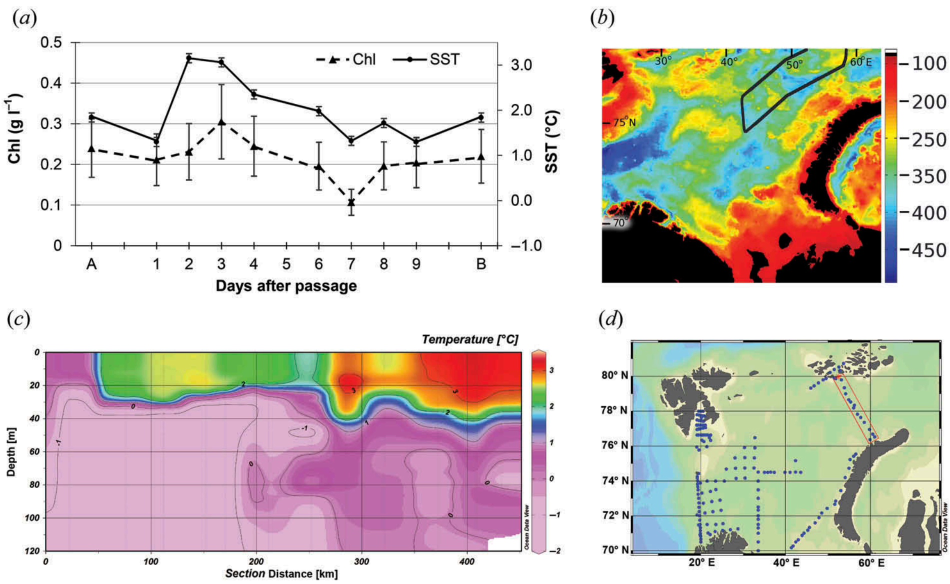

Figure 7. The Barents Sea, 11–12 July 2006. (*a*) Temporal variation in surface chl and SST (spatio-temporal averaging is performed within the cyclone footstep area). Points A and B on the abscissa designate, respectively, days 1–5 prior to cyclone arrival and days 6–10 after cyclone departure. (*b*) Location of the cyclone on the bathymetric map; colourbar is in metres. (*c*) Cross-section of water temperature along a line extending from Franz Josef Land to Novaya Zemlya (i.e. the right-hand side of plate (*d*), which shows the location of the transect (red box)).

In the same vein, the timing of chl maximum formation (see Figure 7(*a*)) was significantly (p < 0.0001) correlated with the H: the coefficient of determination was 0.56 (RMSE = 0.8 (or 47%)),

$$T = 0.89 + 0.0187H. \quad (2)$$

In regard to response of the first type, the cyclone-driven enhancements of chl and SST were in the range (1–2) μg l^{-1} (only rarely reaching 4 μg l^{-1}) and 1°C, respectively.

The pattern of response of the first type (Figure 6) assumes that although the cyclone's arrival led (moment A in Figure 6) to inevitable mixing of surface and subsurface layers, the thermal and productivity levels of water within this stratum are very close. However, over the course of several days the cyclone-induced vertical mixing continued propagating to a lesser extent with the result that a few days after cyclone onset, increased vertical mixing brought deeper waters to the surface. On reaching the surface those deeper waters, being rich in nutrients (Tremblay et al. 2013), represented ideal conditions of both temperature and light availability. A couple of days were required for any appreciable increase in surface PP, which is mirrored by a relatively short-lived spike in chl. The duration of this spike was short: the pool of new nutrient resources was gradually depleted (point B in Figure 6), with chl eventually at pre-cyclone values.

Ekman layer depth (h, m) can be estimated using the following relationship (Chen and Tang 2012):

$$h = 7.12 \times \left[\frac{1}{\sqrt{\sin\varphi}}\right] \times V_{\max}, \tag{3}$$

where φ = latitude (°) and $V_{\max}$ = maximum wind speed (m s^{-1}) at 10 m above sea level within the footprint area.

For the cyclone parameters investigated, h varied between ~100 and ~230 m. These assessments indicate that the BS cyclones were actually capable of acting as Ekman pumps, entraining waters from very significant depths up to the surface.

Analysis of the trajectories of cyclones resulting in the first type of response showed that all were located within the region encompassing currents originating from the intrusion of Atlantic waters through the Barents Gates (point 8 in Figure 1) and propagating to the east across the BS. Generally, these currents reside in the top ~250 m layer (Reigstad et al. 2002) and drive relatively warm and nutrient-enriched waters as compared with both local BS and inflowing Arctic waters.

The suggested mechanism of the first type of response can be further underpinned by considerations based on the Redfield ratio paradigm, according to which the stoichiometric ratio of carbon, nitrogen, and phosphorus (C:N:P) found in phytoplankton throughout the deep oceans is 106:16:1 (Redfield 1934). The BS nutrient pool is known to be strongly nitrogen-limited (Jakobsen and Ozhigin 2011), as exemplified by the results of the field campaigns of two consecutive years conducted by Reigstad et al. (2002) along the Kola Transect: in March (the time when assumingly no consumption does take place, and the nutrient abundance represents true winter concentrations) the N:P ratio in the central BS and the MIZ constituted < 10.4:0.75 as compared with the aforementioned Redfield ratio (16:1), which provides a useful screening criterion.

In the absence of data on biogeochemical shipborne measurements performed during our decadal spaceborne observations of cyclone-driven effects, and in light of reported studies (Jakobsen and Ozhigin 2011; Reigstad et al. 2002), we assume that the BS is putatively N-limited.

Smith (2006), assuming the validity of the Redfield ratio and based on a cross-ecosystem comparison of data obtained from 92 marine coastal zone systems worldwide, established a regression model for putatively N-limited sites. In the case of availability of data on total phosphorus (TP), the regression equation is as follows:

$$\text{logchl} = 0.99\ \log TP + 0.11\ \left(r^2 = 0.74\right). \tag{4}$$

To apply this relationship, we employed the aforementioned Kola Transect shipborne data on TP (Reigstad et al. 2002). The results of our numerical assessments are exemplified in the case displayed in Figure 6 for mid-April and the coastal zone waters of the BS. The value of chl prior to the cyclone onset was about 0.6 μg l^{-1}, and the TP value in surface waters putatively constituted 0.4–0.5 μmolP l^{-1} (Reigstad et al. 2002, their Figure 4(*b*)).

The cyclone impact resulted in an increase in chl-*a* to ~1.0 μg l^{-1}. As a result of associated cyclone-driven vertical mixing (remember that, according to our estimations, the cyclones considered in our study were strong enough to agitate the water column from bottom to surface), the value of TP increased to ~0.7–0.8 μmolP l^{-1}.

The application of Equation (4) to two time periods relating to the situation illustrated in Figure 6, viz. (1) prior to the cyclone arrival and (2) the onset of chl maximum response shows that the calculated values of chl were 0.58 and 0.97 μg l^{-1} as compared with the remotely retrieved values of 0.6 and 1.0 μg l^{-1}, respectively.

Thus, we believe that this example supports our spaceborne interpretation of the nature/mechanism of surface chl modulation as an aftermath of the cyclone passage and the ensuing water column vertical mixing.

Thus, instances of the first type of response are related to the mechanism suggested above – cyclone-induced pumping of nutrient-rich waters of Atlantic origin to the water surface followed by a relatively short-lived enhancement of phytoplankton productivity in the upper layers lasting until the depletion of pools of nutrients brought up from below. The sequence described is illustrated in Figure 6 (plates *a*–*d*). This type of response can be expected to occur within the vast area of Atlantic waters propagating across the southern and central BS (see Figure 2), and explains the prevalence of the first type of response.

Observed only on limited occasions, the second type of response is thought to be associated with situations where some cyclones propagating generally from south to north across the BS eventually reach the PF (their position is illustrated in Figure 4 for a specific year). When meeting the PF zone (compare Figures 4 and 7, plate *b*), the cyclone trajectory overlaps the BS currents of Atlantic origin and a sequence of dynamic processes unfolds. The water of Atlantic origin (its SST profile is illustrated on the right-hand side of plate *c*, Figure 7) plunges under the surface layers of Arctic water – a phenomenon well established for the BS (Jakobsen and Ozhigin 2011). Because of subduction, warmer and more nutrient-rich waters are then located beneath a 'blanket' of cold Arctic water. With the arrival of the cyclone, the submerged Atlantic water is raised to the surface due to the aforementioned Ekman pumping mechanism. Within 1–2 days the propulsion of submerged waters is manifested (see Figure 7, plate *a*) through the enhancement of both chl and SST. However, within a few days this temporary dual increase weakens, thermal and biological levels eventually returning to their initial values (point A in plate *a*, Figure 7). We do not have any substantiated explanation for the minima in chl and SST that occurred on the seventh day in that specific example. In other observed cases of the second type response this feature did not appear.

7. Concluding remarks

The results obtained from the present study indicate that the passage of cyclones at high northern latitudes (with the BS as an example) results in a temporary enhancement of phytoplankton chl, which is widely considered as a proxy of the primary productivity level (e.g. Kirk 1983).

However, this general statement does not imply a close similarity between the major features of response of high- and low-latitude waters to cyclone impacts (for the latter see Section 2).

The *common* features are: (1) cyclones modify 2D thermal and hydrobiological fields along the footstep trajectory; (2) the major impact is produced by cyclones with the highest depression depth and low translation speed; and (3) a more intense surface chl enhancement (up to 25%) was observed on the right-hand side of the footprint stripe, as supported by previous studies in the northern hemisphere (e.g. Son et al. 2007).

The major *specific* features are the following: (1) there are two types of response to cyclone impact in the BS – surface chl can increase but, in some specific instances, may decrease while SST can remain either nearly intact or even increase; (2) surface chl and SST increase is a short-term phenomenon (its duration is between a few days and two weeks); and (3) the *absolute* values of cyclone-induced Δchl and, especially ΔSST, are much lower than those generally reported for low latitudes (see Section 2).

Regarding the total *seasonal* impact of cyclones on PP in the BS, it should be borne in mind that (1) the number of cyclones per vegetation season suitable for study by ocean colour sensors proved to be generally about 2–3 or even less (as compared with the total seasonal number); (2) increase in chl due to the cyclone impact covers a wide range (on average, 0.2 μg l^{-1} and never exceeding ~0.4 μg l^{-1}); and (3) the average cumulative area covered by a translating footprint generally accounts for about 14% of the BS area. Also, it should be taken into account that the rate of PP is markedly less in the footprint *cloudy* areas than in *sunlit* areas in the wake of the translating cyclone.

All the above limitations/uncertainties prevent any quantified assessment of the actual impact of cyclones on PP of the BS based solely on 23 cases. However at the qualitative level, our data seem to imply that cyclones are hardly essential boosters of PP in the BS.

A further substantiation of the above corollary concerning the influence of cyclones on chl was obtained through a dedicated correlation analysis performed for 96 cyclones occurring over the vegetation period during the 11-year study (see Figure 3). The repartition of 96 cyclones across the spaceborne observation period was compared to the respective inter-annual variation in chl obtained in this study from satellite data and averaged over the ice-free BS area. This analysis yielded a coefficient of correlation as low as 0.35 (level of significance $p > 0.1$). We are of the opinion that because the data analysed include not only those cases amenable to optical remote sensing (i.e. 23 relatively cloud-free), but also cloudy cases unsuitable for optical remote sensing, the results thus obtained better reflect the cause-and-effect correspondence we were investigating. That is why we believe that this is a more robust argument in favour of our above assumption that the inter-annual variation in chl across the BS can be only peripherally affected by passing cyclones. Obviously, other multiple forcing factors collectively control the observed inter-annual variation in chl averaged over the BS.

It could be conjectured that the same conclusion might be made with respect to the pelagic Arctic tracts, which are generally even less productive than the BS (Petrenko et al.

2013) and for which cloudiness during the vegetation season is very frequent, heavy, and extends over immense areas. However, this supposition certainly requires further study in order to advance our understanding of the actual role of cyclones in modulations of Arctic Ocean productivity and ecosystem functioning.

Acknowledgement

The authors wish to express their gratitude to Dr Vladimir Volkov for valuable discussions of the research results.

Disclosure statement

No potential conflict of interest was reported by the authors.

Funding

The present study was initiated under a joint Russian–Chinese Project [12-05-91170-ГФУР_а, no 01201255442, NSFC–RFBR-41211120181], 'Investigation of factors driving changes in phytoplankton surficial fields as an aftermath of passage of hurricanes in tropical and polar regions' (1 January 2012 to 31 December 2013). The authors express their gratitude to the Russian Foundation for Basic Research (RFBS) and Key Programme of the National Natural Science Foundation of China (NSFC 41430968) for financial support.

References

Akmaykin, D. A., O. A. Bukin, P. A. Permyakov, and P. A. Salyuik. 2013. "Assessments of the Tropical Cyclone Influence on Chlorophyll-A Fields in Some Regions of the Pacific." In *Proceedings of the Remote Sensing of Environment: Scientific and Applied Research in Asia-Pacific International Conference (RSAP2013)*, September 24–27, edited by P. A. Permyakov, 33. Vladivostok: Institute of Automation and Control Process, Far Eastern Branch, Russian Academy of Sciences.

Arrigo, K., D. K. Perovich, R. S. Pickart, Z. W. Brown, G. L. van Dijken, K. E. Lowry, M. M. Mills, M. A. Palmer, W. M. Balch, F. Bahr, N. R. Bates, C. Benitez-Nelson, B. Bowler, E. Brownlee, J. K. Ehn, K. E. Frey, R. Garley, S. R. Laney, L. Lubelczyk, J. Mathis, A. Matsuoka, B. G. Mitchell, G. W. K. Moore, E. Ortega-Retuerta, S. Pal, C. M. Polashenski, R. A. Reynolds, B. Schieber, H. M. Sosik, M. Stephens, and J. H. Swift. 2012. "Massive Phytoplankton Blooms Under Arctic Sea Ice." *Science* 336: 1408. doi:10.1126/science.1215065.

Arrigo, K., and G. van Dijken. 2011. "Secular Trends in Arctic Ocean Net Primary Production." *Journal of Geophysical Research* 116 (C9): 1−15. doi:10.1029/2011JC007151.

Babin, S. M., J. A. Carton, T. D. Dickey, and J. D. Wiggert. 2004. "Satellite Evidence of Hurricane-Induced Phytoplankton Blooms in an Oceanic Desert." *Journal of Geophysical Research* 109: C03043. doi:10.1029/2003JC001938.

Bélanger, S., M. Babin, and J.-É. Tremblay. 2013. "Increasing Cloudiness in Arctic Damps the Increase in Phytoplankton Primary Production Due to Sea Ice Receding." *Biogeosciences* 10: 4087–4101. doi:10.5194/bg-10-4087-2013.

Bobylev, L. P., K. Y. Kondratyev, and O. M. Johannessen. 2003. *Arctic Environment Variability in the Context of Global Change*, 470pp. Chichester: Springer-Praxis.

Byju, P., and P. S. Kumar. 2011. "Physical and Biological Response of the Arabian Sea to Tropical Cyclone Phyan and Its Implications." *Marine Environmental Research* 71 (5): 325–330. doi:10.1016/j.marenvres.2011.02.008.

Callahan, P. S., and T. Lungu. 2006. *QuikSCAT Science Data Product User's Manual (v3.0)*, 91. Pasadena, CA: Jet Propulsion Laboratory.

Chang, J., C.-C. Chung, and G.-C. Gong. 1996. "Influences of Cyclones on Chlorophyll a Concentration and *Synechococcus* Abundance in a Subtropical Western Pacific Coastal Ecosystem." *Marine Ecology Progress Series* 140: 199–205. doi:10.3354/meps140199.

Chen, Y., and D. L. Tang. 2012. “Eddy-Feature Phytoplankton Bloom Induced by a Tropical Cyclone in the South China Sea.” *International Journal of Remote Sensing* 33 (23): 7444–7457. doi:10.1080/01431161.2012.685976.

Chernokulsky, A., and T. I. Mokhov. 2012. “Climatology of Total Cloudiness in the Arctic: An Interpretation of Observations and Reanalysis.” *Advances in Meteorology* 2012: 1–15. doi:10.1155/2012/542093.

Chung, C.-C., G.-C. Gong, and C.-C. Hung. 2012. “Effect of Typhoon Morakot on Microphytoplankton Population Dynamics in the Subtropical Northwest Pacific.” *Marine Ecology Progress Series* 448: 39–49. doi:10.3354/meps09490.

Dare, R. A., and J. L. McBride. 2011. “Sea Surface Temperature Response to Tropical Cyclones.” *Monthly Weather Review* 139: 3798–3808. doi:10.1175/MWR-D-10-05019.1.

Davis, A., and X.-H. Yan. 2004. “Hurricane Forcing on Chlorophyll-A Concentration off the Northeast Coast of the U.S.” *Geophysical Research Letters* 31: LI 7304. doi:10.1029/2004GL020668.

Engelsen, O., E. N. Hegseth, H. Hop, E. Hansen, and S. Falk-Petersen. 2002. “Spatial Variability of Chlorophyll-A in the Marginal Ice Zone of the Barents Sea, with Relations to Sea Ice and Oceanographic Conditions.” *Journal of Marine Systems* 35: 79–97. doi:10.1016/S0924-7963(02)00077-5.

Gaston, R. W., and F. Rodriguez. 2008. *Quikscat Follow-On Concept Study*. Pasandena, CA: Jet Propulsion Laboratory, NASA Publications (http://hdl.handle.net/2014/40793).

Grebmeir, J. M., J. E. Overland, S. E. Moore, E. V. Farley, E. C. Carmack, L. W. Cooper, K. E. Frey, J. H. Helle, F. A. McLaughlin, and S. McNutt. 2006. “A Major Ecosystem Shift in the Northern Bering Sea.” *Science* 311: 1461–1463. doi:10.1126/science.1121365.

Greene, C., and A. Pershing. 2007. “OCEANS: Climate Drives Sea Change.” *Science* 315 (5815): 1084–1085. doi:10.1126/science.1136495.

Hanshaw, M. N., M. S. Lozier, and J. B. Palter. 2008. “Integrated Impact of Tropical Cyclones on Sea Surface Chlorophyll in the North Atlantic.” *Geophysical Research Letters* 35: LOl60l. doi:10.1029/2007GL031862.

Hosoda, K., H. Murakami, F. Sakaida, and H. Kawamura. 2007. “Algorithm and Validation of Sea Surface Temperature Observation Using MODIS Sensors Aboard Terra and Aqua in the Western North Pacific.” *Journal of Oceanography* 63: 267–280. doi:10.1007/s10872-007-0027-4.

Jakobsen, T., and V. K. Ozhigin, eds. 2011. *The Barents Sea: Ecosystem, Resources, Management*, 825 pp. Trondheim: Tapir Academic Press.

Jullien, S., C. E. Menkes, P. Marchesiello, N. C. Jourdain, M. Lengaigne, A. Koch-Larrouy, J. Lefèvre, E. M. Vincent, and V. Faure. 2012. “Impact of Tropical Cyclones on the Heat Budget of the South Pacific Ocean.” *Journal of Physical Oceanography* 42: 1882–1906. doi:10.1175/JPO-D-11-0133.1.

Kalnay, E., M. Kanamitsu, R. Kistler, W. Collins, D. Deaven, L. Gandin, M. Iredell, S. Saha, G. White, J. Woollen, Y. Zhu, A. Leetmaa, R. Reynolds, M. Chelliah, W. Ebisuzaki, W. Higgins, J. Janowiak, K. C. Mo, C. Ropelewski, J. Wang, R. Jenne, and D. Joseph. 1996. “The NCEP/NCAR 40-Year Reanalysis Project.” *Bulletin of the American Meteorological Society* 77: 437–471. doi:10.1175/1520-0477(1996)077<0437:TNYRP>2.0.CO;2.

Kawai, Y., and A. Wada. 2011. “Detection of Cyclone-Induced Rapid Increases in Chlorophyll A with Sea Surface Cooling in the Northwestern Pacific Ocean from a Modis/Seawifs Merged Satellite Chlorophyll Product.” *International Journal of Remote Sensing* 32 (24): 9455–9471. doi:10.1080/01431161.2011.562252.

Kirk, J. T. O. 1983. *Light and Photosynthesis in Aquatic Ecosystems*, 401 pp. Melbourne: Cambridge University Press.

Knutson, T., J. L. McBride, J. Chan, K. Emanuel, G. Holland, C. Landsea, I. Held, J. P. Kossin, A. K. Srivastava, and M. Sugi. 2010. “Tropical Cyclones and Climate Change.” *Nature Geoscience* 3: 157–163. doi:10.1038/ngeo779.

Korosov, A. A., D. V. Pozdnyakov, A. Folkestad, L. H. Pettersson, K. Sørensen, and R. Shuchman. 2009. “Semi-Empirical Algorithm for the Retrieval of Ecology-Relevant Water Constituents in Various Aquatic Environments.” *Algorithms* 2: 470–497. doi:10.3390/a2010470.

Le Fouest, V., C. Postlethwaite, M. A. Morales Maqueda, S. Bélanger, and M. Babin. 2011. “On the Role of Tides and Strong Wind Events in Promoting Summer Primary Production in the Barents Sea.” *Continental Shelf Research* 31: 1869–1879. doi:10.1016/j.csr.2011.08.013.

Leipper, D. F. 1967. “Observed Ocean Conditions and Hurricane Hilda, 1964.” *Journal of the Atmospheric Sciences* 24: 182–186. doi:10.1175/1520-0469(1967)024<0182:OOCAHH>2.0.CO;2.

Lin, I. 2012. “Typhoon-Induced Phytoplankton Blooms and Primary Productivity Increase in the Western North Pacific Subtropical Ocean.” *Journal of Geophysical Research* 117: C03039. doi:10.1029/2011JC007626.

Lin, I., W. T. Liu, C.-C. Wu, G. T. F. Wong, C. Hu, Z. Chen, W.-D. Liang, Y. Yang, and K.-K. Liu. 2003. “New Evidence for Enhanced Ocean Primary Production Triggered by Tropical Cyclone.” *Journal of Geophysical Research. Letters* 30 (13): 1718–1723. doi:10.1029/2003GL017141.

Loeng, H., and K. Drinkwater. 2007. “An Overview of the Ecosystems of the Barents and Norwegian Seas and Their Response to Climate Variability.” *Deep Sea Research Part II: Topical Studies in Oceanography* 54: 2478–2500. doi:10.1016/j.dsr2.2007.08.013.

Morozov, E. 2013. “Algorithms for Identification of *Lepidodinium chlorophorum* and *Emiliania huxleyi* in Satellite Images.” PhD diss., Russian State Hydrometeorological University, St. Petersburg, 225pp.

Morozov, E., D. Pozdnyakov, T. Smyth, V. Sychev, and H. Grassl. 2013. “Spaceborne Study of Seasonal, Multi-Year and Decadal Phytoplankton Dynamics in the Bay of Biscay: Geophysical Forcing at Different Time and Space Scales.” *International Journal of Remote Sensing* 34 (4): 1297–1331. doi:10.1080/01431161.2012.718462.

NOAA ATLAS. 2004. “Climatic Atlas of the Arctic Seas 2004.” ftp://ftp.nodc.noaa.gov/pub/data.nodc/woa/PUBLICATIONS/english58.pdf

NODC (NOAA OCEANOGRAPHIC CENTER). 2014. http://www.nodc.noaa.gov/cgi-bin/OC5/NPclimatology/arcticFigurepl

O’Reilly, J., E. S. Maritorena, B. G. Mitchell, D. A. Siegel, K. L. Carder, S. A. Garver, M. Kahru, and C. McClain. 1998. “Ocean Color Chlorophyll Algorithms for Seawifs.” *Journal of Geophysical Research* 103: 24937–24953. doi:10.1029/98JC02160.

O’Reilly, J. E., S. Maritorena, M. C. O’Brien, D. A. Siegel, D. Toole, D. Menzies, R. C. Smith, J. L. Mueller, B. G. Mitchell, M. Kahru, F. P. Chavez, P. Strutton, G. F. Cota, S. B. Hooker, C. R. McClain, K. L. Carder, F. Müller-Karger, L. Harding, A. Magnuson, D. Phinney, G. F. Moore, J.s Aiken, K. R. Arrigo, R. Letelier, and M. Culver. 2000. “SeaWiFS Postlaunch Calibration and Validation Analyses, Part 3.” *NASA Tech. Memo. 2000-206892*, 11, edited by S. B. Hooker and E. R. Firestone, 49 pp. Greenbelt, MD: NASA Goddard Space Flight Center.

Pabi, S., G. L. van Dijken, and K. R. Arrigo. 2008. “Primary Production in the Arctic Ocean, 1998–2006.” *Journal of Geophysical Research* 113: C08005. doi:10.1029/2007JC004578.

Permyakov, M. S., D. A. Akmaykin, P. A. Salyuk, T. I. Tarkhanova, and P. V. Smolin. 2005. “Influence of Typhoons on Phytoplankton Chlorophyll Fields as Revealed from Seawifs Data.” *Earth Observation and Remote Sensing* 5: 56–62. in Russian.

Petrenko, D., D. Pozdnyakov, J. Johannessen, F. Counillon, and V. Sychov. 2013. “Satellite Derived Multi-Year Trend in Primary Production in the Arctic Ocean.” *International Journal of Remote Sensing* 34: 3903–3937. doi:10.1080/01431161.2012.762698.

Price, J. F., T. B. Sandford, and G. Z. Forritall. 1994. “Forced Stage Response to a Moving Hurricane.” *American Meteorological Society* 24 (2): 233–260.

Rao, K. H., A. Smith, and M. M. Ali. 2006. “A Study on Cyclone Induced Productivity in South-Western Bay of Bengal during November–December 2000 Using MODTS (SST and Chlorophyll-*A*) and Altimeter Sea Surface Height Observations.” *Indian Journal of Marine Sciences* 35 (2): 153–160.

Redfield, A. C. 1934. “On the Proportions of Organic Derivations in Sea Water and Their Relation to the Composition of Plankton.” In *James Johnstone Memorial Volume*, edited by R. J. Daniel, 177–192. Liverpool: University Press of Liverpool.

Reigstad, M., P. Wassmann, C. Riser, W. S. Øygarden, and F. Rey. 2002. “Variations in Hydrography, Nutrients and Chlorophyll A in the Marginal Ice-Zone and the Central Barents Sea.” *Journal of Marine Systems* 38: 9–29. doi:10.1016/S0924-7963(02)00167-7.

Robinson, I. S. 1994. *Satellite Oceanography: An Introduction for Oceanographers and Remote Sensing Scientists*, 455 pp. Chichester: Praxis Publishing.

Robinson, I. S. 2004. *Measuring the Oceans from Space the Principles and Methods of Satellite Oceanography*, 675 pp. Berlin: Springer-Praxis.

Salyuk, P. A., I. A. Golik, and I. E. Stepochkin. 2014. “Tropical Cyclones Influence on Bioproductivity of the North-Western Pacific.” *Asia-Pacific Journal of Marine Science and Education* 4 (1): 111–117.

Sarangi, R. K. 2011. "Impact of Cyclones on the Bay of Bengal Chlorophyll Variability Using Remote Sensing Satellites." *Indian Journal of Geo-Marine Sciences* 40 (6): 794–80I.

Siswanto, E., J. Ishizaka, M. Toratani, T. Hirawake, and S.-I. Saitoh. 2007. "The Effect of Tropical Cyclone on the Primary Production Enhancement: Some Results from the W-PASS (Western Pacific Are-Sea Interaction Study) Project." In *Proceedings of the PICES MONITOR/BIO Workshop 5*, October 27, edited by E. A. Pakhomov and O. Yamamura. Vladivostok: Biological Oceanography Committee.

Skagseth, Ø., T. Furevivik, R. Ingvaldsen, H. Loeng, K. A. Mork, K. A. Orvik, and V. Ozigin. 2008. "Volume and Heat Transports to the Arctic Ocean via the Norvegian and Barents Sea." In *Arctic and Subarctic Ocean Fluxes*, edited by R. R. Dickson, J. Meincke, and P. Rhines, 45–64. Springer-Science + Business Media. B. V.

Smith, V. H. 2006. "Responses of Estuarine and Coastal Marine Phytoplankton to Nitrogen and Phosphorus Enrichment." *Limnology and Oceanography* 51 (I, part 2): 377–384. doi:10.4319/lo.2006.51.1_part_2.0377.

Smyth, T., T. Tyrrel, and B. Tarrant. 2004. "Time Series of Coccolithophore Activity in the Barents Sea, from Twenty Years of Satellite Imagery." *Geophysical Research Letters* 31 (L11302): 1–4. doi:10.1029/2004GL019735.

Son, S., T. Platt, C. Fuentes-Yaco, H. Bouman, E. Devred, Y. Wu, and S. Sathyendranath. 2007. "Possible Biogeochemical Response to the Passage of Hurricane Fabian Observed by Satellites." *Journal of Plankton Research* 29 (8): 687–697. doi:10.1093/plankt/fbm050.

Sterckx, S., E. Knaeps, and K. Ruddick. 2011. "Detection and Correction of Adjacency Effects in Hyperspectral Airborne Data of Coastal and Inland Waters: The Use of the near Infrared Similarity Spectrum." *International Journal of Remote Sensing* 32 (21): 6479–6505. doi:10.1080/01431161.2010.512930.

Tang, D. L., H. Kawamura, T. V. Dien, and M. A. Lee. 2004a. "Offshore Phytoplankton Biomass Increase and Its Oceanographic Causes in the South China Sea." *Marine Ecology Progress Series* 268: 31–41. doi:10.3354/meps268031.

Tang, D. L., H. Kawamura, H. Doan-Nhu, and W. Takahashi. 2004b. "Remote Sensing Oceanography of a Harmful Algal Bloom off the Coast of Southeastern Vietnam." *Journal of Geophysical Research* 109: C03014. doi:10.1029/2003JC002045.

Tang, D. L., H. Kawamura, P. Shi, W. Takahashi, L. Guan, T. Shimada, F. Sakaida, and O. Isoguchi. 2006. "Seasonal Phytoplankton Blooms Associated with Monsoonal Influences and Coastal Environments in the Sea Areas either Side of the Indochina Peninsula." *Journal of Geophysical Research* 111: GOI0I0. doi:10.1029/2005JG000050.

Tang, D. L., and G. J. Sui, eds. 2014. *Typhoon Impact and Crisis Management*, 578 pp. Heidelberg: Springer Science + Business Media.

Thiersten, H., and J. Young. 2004. *Coccolithophores – From Molecular Processes to Global Impact*. Berlin: Springer-Verlag.

Toratani, M. 2008. "Primary Production Enhancement by Typhoon Ketsana in 2003 in Western North Pacific." *Remote Sensing of Inland, Coastal, and Oceanic Waters, Proceedings. SPIE* 7150: 1–3.

Tremblay, J.-É., P. Raimbault, N. Garcia, B. Lansard, M. Babin, and J. Gagnon. 2013. "Impact of River Discharge, Upwelling and Vertical Mixing on the Nutrient Loading and Productivity of the Canadian Beaufort Shelf." *Biogeosciences Discussions* 10: 16675–16712. doi:10.5194/bgd-10-16675-2013.

Walker, N. D., R. R. Leben, and S. Balasubramanian. 2005. "Hurricane-Forced Upwelling and Chlorophyll a Enhancement within Cold-Core Cyclones in the Gulf of Mexico." *Geophysical Research. Letters* 32: LI8610. doi:10.1029/2005GL023716.

Webster, P. J., G. J. Holland, J. A. Curry, and H.-R. Chang. 2005. "Changes in Tropical Cyclone Number, Duration, and Intensity in a Warming Environment." *Science* 309 (5742): 1844–1846. doi:10.1126/science.1116448.

Ying, M., T. R. Knutson, H. Kamahori, and T.-C. Lee. 2012. "Impacts of Climate Change on Tropical Cyclones in the Western North Pacific Basin. Part II: Late Twenty-First Projections." *Tropical Cyclone Research and Review* 1 (2): 231–241.

Yu, B. V. 2009. *Space and Time Variability of Hydrophysical Fields in the Ocean*, 320 pp. St. Petersburg: Russian Ministry of Natural Resources.

Yu, J., D. L. Tang, Y. Li, Z. Huang, and G. Chen. 2013. "Increase in Fish Abundance during Two Typhoons in the South China Sea." *Advances in Space Research* 51 (9): 1734–1749. doi:10.1016/j.asr.2012.11.019.

Zhao, H., and D. L. Tang. 2006. "The Spatial Distribution of Chlorophyll-A and Its Responses to Oceanographic Environments in the South China Sea." *Advances in Geosciences* 5: 7–14.

Zhao, H., D. L. Tang, and D. Wang. 2009. "Phytoplankton Blooms near the Pearl River Estuary Induced by Typhoon Nuri." *Journal of Geophysical Research* 114: C12027. doi:10.1029/2009JC005384.

Zhao, H., D. L. Tang, and Y. Wang. 2008. "Comparison of Phytoplankton Blooms Triggered by Two Typhoons with Different Intensities and Translation Speeds in the South China Sea." *Marine Ecology Progress Series* 365: 57–65. doi:10.3354/meps07488.

Zheng, G. M., and D. L. Tang. 2007. "Offshore and Nearshore Chlorophyll Increases Induced by Typhoon Winds and Subsequent Terrestrial Rainwater Runoff." *Marine Ecology Progress Series* 333: 61–74. doi:10.3354/meps333061.